

**A NEW MECHANISTIC MODEL FOR MIC  
BASED ON A BIOCATALYTIC CATHODIC SULFATE REDUCTION THEORY**

Tingyue Gu (Speaker), Kaili Zhao, Srdjan Nestic  
Department of Chemical and Biomolecular Engineering  
and Institute for Corrosion and Multiphase Technology  
Ohio University, Athens, Ohio 45701  
gu@ohio.edu

**ABSTRACT**

Microbiologically induced corrosion (MIC) due to sulfate-reducing bacteria (SRB) is a major problem facing the oil and gas industry as well as other industries such as water utility. Current risk-factor probability models are useful in predicting the likelihood of MIC. However the reliable prediction of the progression of MIC pitting must depend on mechanistic modeling. This paper presents a mechanistic model for the prediction of MIC pitting progression based on a biocatalytic cathodic sulfate reduction (BCSR) theory. The hydrogenase system in the sessile SRB cells at the interface of biofilm and metal surface is treated as a bio-electrocatalyst for sulfate reduction. The model considers both charge transfer resistance and mass transfer resistance. It can be calibrated using an experimentally measured electrochemical parameter recast as “biofilm aggressiveness” for a particular SRB biofilm. Other charge transfer and mass transfer parameters are used as available in the literature or from existing experimental correlations. Computer simulation indicates that charge transfer resistance is important initially when the biofilm thickness is small. However, mass transfer resistance becomes dominant after pit grows to a sizable depth. In fact, the growth of any deep pits will always be mass transfer controlled regardless of how aggressive the biofilm is.

Keywords: mechanistic MIC model, charge transfer, mass transfer, sulfate reduction, SRB

Copyright

©2009 by NACE International. Requests for permission to publish this manuscript in any form, in part or in whole must be in writing to NACE International, Copyright Division, 1440 South creek Drive, Houston, Texas 777084. The material presented and the views expressed in this paper are solely those of the author(s) and are not necessarily endorsed by the Association. Printed in the U.S.A.

## INTRODUCTION

Microbiologically induced corrosion (MIC) is a major problem in the oil and gas industry. A group of bacteria known as sulfate reducing bacteria (SRB) are often found to be the cause<sup>1</sup>. Other bacteria such as acid producing bacteria (APB) can also cause MIC. Noncorrosive bacteria may form synergistic consortia with corrosive bacteria. Current MIC models are risk factor models that predict the likelihood of MIC. Such models are useful in practice to a limited extent because they are unable to predict MIC progression accurately. A mechanistic model is needed. One prevailing theory in MIC due to SRB is the so-called cathodic depolarization theory (CDT)<sup>2,3</sup> hinging on SRB hydrogenase to convert the adsorbed hydrogen atoms (formed by the cathodic reduction of proton) on the cathode to hydrogen and then to H<sup>+</sup>, thus pushing the cathodic reduction of proton reaction forward. This reaction removes the electrons generated by iron dissolution. Costello<sup>4</sup>, however, proposed that hydrogen sulfide H<sub>2</sub>S, rather than H<sup>+</sup> could act as cathodic reactant, i.e.,

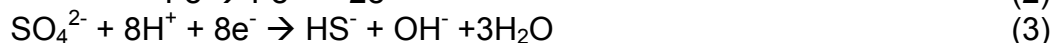


A number of other studies<sup>5-7</sup> also showed that sulfate reduction could occur successively even with the hydrogen formation on the cathodic site.

## A NEW MECHANISTIC MIC MODEL

### Biocatalytic Electrochemistry

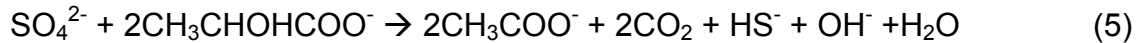
This work presents a mechanistic model based on a biocatalytic cathodic sulfate reduction (BCSR) theory<sup>8</sup> for MIC due to SRB. This theory assumes that MIC occurs because the electrons released by iron dissolution at the anode are utilized in the sulfate reduction at the cathode. The actual cathodic reactions are more complex, but this theory considers only the overall effect.



Reaction 3 normally happens at a negligible rate without biocatalysis from biofilms. The reaction is catalyzed by the hydrogenase enzyme system of hydrogenase-positive SRB cells that is responsible for accelerated sulfate reduction<sup>9</sup>. Some hydrogen sulfide ion (HS<sup>-</sup>) will convert to hydrogen sulfide, especially in acidic pH. A sulfide film is often found under an SRB biofilm on a metal surface while other metal surface areas not covered by the biofilm do not have it.



It is well known to cell biologists that dissimilatory sulfate reduction with concomitant carbon source (such as acetate and lactate) oxidation provides energy for anaerobic SRB metabolism. SRB cells can live as planktonic cells. Sulfate reduction by these cells uses electrons donated by oxidation of a carbon source such as lactate as shown below,



SRB cells colonize solid surfaces by forming biofilms. They can attach to metal, plastic and even glass surfaces. Their survival is enhanced by doing so because biofilms are protective against harsh elements such as biocide attacks and pH swings in the bulk fluid phase. It is also possible that sessile SRB cells benefit by living synergistically with other sessile cells in the same biofilm consortium that provides them with a better nutritional environment and a protection shield. When sessile SRB cells reside on an iron surface, their hydrogenase enzyme system catalyzes cathodic sulfate reduction by accepting electrons donated by iron dissolution, thus promoting corrosion.

It should be understood that not all sessile cells in a biofilm participate directly in the catalysis of cathodic sulfate reduction. Only those at the interface of the biofilm and metal surface have a direct impact on MIC, because water and cells are poor electron conductors. It is known in biofilm catalysis that once a biofilm is mature, its catalytic ability will level off<sup>10</sup>. Maturity in this case is achieved when the cell surface-density at the interface of biofilm and metal surface reaches its peak. A thicker biofilm does not necessarily mean a better biocatalytic performance at the interface. In fact, a thicker biofilm may actually hinder cathodic reactions because of increased mass transfer resistance presented by the biofilm.

Planktonic cells may or may not contribute to corrosion. For SRB corrosion, planktonic and sessile cells both can produce H<sub>2</sub>S. The H<sub>2</sub>S produced by planktonic cells can diffuse through the biofilm and reach the metal surface causing H<sub>2</sub>S corrosion. Due to dilution by the bulk fluid, the contribution from planktonic cells to the local concentration at the metal surface may be small compared to the locally produced H<sub>2</sub>S by sessile cells. This is supported by the fact that in the absence of an SRB biofilm, pitting is not observed in the laboratory. APB should have a similar situation regarding the corrosive acids they produced compared to the H<sub>2</sub>S produced by SRB. For simplicity in modeling, it is assumed that the bulk-fluid phase concentrations of corrosive species are constant. This would include the contribution of planktonic cells to the amount of corrosive chemicals in the form of increased bulk-fluid phase concentrations.

A key equation in electrochemistry is the Butler-Volmer describing electrical current relationship to the electrode potentials. Both anodic and cathodic electrical current on the same electrode can be expressed by the equation:

$$i = i_0 \cdot \left\{ \exp \left[ \frac{(1-\alpha) \cdot n \cdot F}{R \cdot T} \cdot (E - E_{\text{eq}}) \right] - \exp \left[ - \frac{\alpha \cdot n \cdot F}{R \cdot T} \cdot (E - E_{\text{eq}}) \right] \right\} \quad (6)$$

*i*: electrode current density, A/m<sup>2</sup>

*i*<sub>0</sub>: exchange current density, A/m<sup>2</sup>

*E*: electrode potential, V

*E*<sub>eq</sub>: equilibrium (standard) potential, V

*T*: absolute temperature, K

*n*: number of electrons involved in an electrodic reaction

*F*: Faraday constant

*R*: universal gas constant

*α*: symmetry factor, dimensionless

In high overpotential situations, the Butler-Volmer equation simplifies to the common Tafel equation. In the electrochemical corrosion process, iron dissolution is the only anodic reaction and it is always under charge transfer control. Tafel equation is used to calculate the current

density of anodic iron oxidation. There are several possible cathodic reduction reactions including  $H^+$  reduction, sulfate reduction, and acetic acid reduction. The overall resistance for each cathodic reduction reaction can be expressed as the sum of charge transfer resistance and mass transfer resistance. Tafel equation is used to describe charge transfer resistance, and the film mass transfer theory is used to calculate mass transfer resistance<sup>8</sup>.

The ability to facilitate cathodic sulfate reduction can be viewed as the aggressiveness factor of a biofilm. The biofilm aggressiveness is strongly dependent on SRB species, their metabolic environment and sessile SRB surface density on the cathode. This parameter is equivalent to the reaction rate constant in chemical reactions. Thus, it is independent of mass transfer. This is very useful in guiding SRB lab experiments. The biofilm aggressiveness can be easily used to calibrate the model. Other electrochemical parameters are readily available from literature. The anodic current density is equal to the overall cathodic current density.

$$i_{a(Fe)} = i_{c(H^+)} + i_{c(H_2CO_3)} + i_{c(organic\_acid)} + i_{c(SO_4^{2-})} \quad (7)$$

## Mass Transfer Mechanism

As shown in Figure 1, a corrosive chemical species migrating toward or away from an iron surface must diffuse through both the aqueous and biofilm layers, resulting in concentration gradients due to mass transfer resistances. In a real world, SRB biofilm often resides underneath another biofilm synergistically. The top biofilm sometimes is an aerobic biofilm that consumes oxygen providing an anaerobic local environment for SRB. According to Grady<sup>11</sup>, mass transfer resistance in the liquid layer outside the biofilms was found to be minimal when the bulk fluid was well agitated, and moreover, Bailey and Ollis<sup>12</sup> calculated the Biot number for a biofilm system and found it to be larger than 200 meaning a very strong dominance of biofilm resistance to mass transfer. Therefore, the external mass transfer resistance is limited to the biofilm layer with negligible diffusion resistance in the bulk fluid. This means the concentration of a chemical species at the surface of the top biofilm is equal to  $C_b$  (bulk-fluid phase concentration) in Figure 1. On the iron surface, some parts may be passivated due to the formation of a protective iron sulfide film. The same may happen to some pit bottom surfaces leading to dead pits. It is those non-passivated pits that keep growing eventually causing pinhole leaks. This model will calculate the pitting corrosion rate and the largest pit depth without passivation.

To calculate mass transfer resistance, diffusion coefficients for corrosive chemical species are needed. Literature data on diffusivity are typically for diffusion in aqueous media, not in biofilms. The diffusion coefficients of each species within biofilm can be determined by the following relationship<sup>13</sup>, which shows that diffusivity in biofilm is related to the biofilm density. Aqueous diffusivity  $D_w$  of each species is available in the literature.

$$\frac{D}{D_w} = 1 - \frac{0.43X^{0.92}}{11.19 + 0.27X^{0.99}} \quad (8)$$

D: effective diffusivity in the biofilm ( $m^2/s$ ) to be used in our model

$D_w$ : diffusivity in aqueous liquid without biofilm ( $m^2/s$ )

X: biofilm density,  $mg/cm^3$

In an SRB system, soluble species such as,  $Fe^{2+}$ ,  $SO_4^{2-}$ ,  $H^+$ ,  $OH^-$  and  $H_2S$  that are involved in corrosion process have a concentration distribution in biofilms. The concentration distribution

of each species across each biofilm layer is governed by the following diffusion equation from mass balance.

$$\frac{\partial C_j}{\partial t} = \frac{\partial}{\partial x} \left( D_j \frac{\partial C_j}{\partial x} \right) + R_j \quad (9)$$

$C_j$ : concentration of chemical species  $j$  in biofilm, mol/m<sup>3</sup>

$D_j$ : diffusion coefficient for species  $j$ , m<sup>2</sup>/s

$R_j$ : rate of consumption of species  $j$  by sessile cells in the bulk of biofilm, mol/ (m<sup>3</sup>·s)

For SRB,  $R$  will be a negative value indicating consumption of sulfate by the bulk sessile cells in the biofilm. The For APB,  $R$  will be a positive value because an acid is produced throughout the biofilm. This mass transfer equation and all the electrochemical equations can be solved numerically with some simplifications to provide corrosion potential and current density  $i_{a(Fe)}$  at different times. The corrosion current density is equal to the anodic current density,  $i_{a(Fe)}$ , that can be converted to corrosion rate CR (pitting rate in this work) based on the following equation,

$$CR = \frac{M_{Fe}}{2F\rho_{Fe}} i_{a(Fe)} \quad (10)$$

After substituting the molecular weight and density for iron, Eq. 10 can be expressed as<sup>14</sup>,

$$CR \text{ (mm/y)} = 1.155 i_{a(Fe)} \text{ (A/m}^2\text{)} \quad (11)$$

Because H<sub>2</sub>S corrosion is non-electrochemical, it does not contribute to the overall cathodic current. It should be added to the CR value calculated from Eq. 11 directly.

## RESULTS AND DISCUSSION

The BCSR model system of equations has been solved numerically to develop MIC prediction software. MICORP Version 1 with windows graphic user interface is the most basic version. Using typical electrochemical and mass transfer parameters<sup>8</sup> (including 5x10<sup>-10</sup> m<sup>2</sup>/s for sulfate diffusivity in biofilms, 28 mM for seawater sulfate concentration, and 50 micron SRB biofilm) at 25°C and a biofilm aggressiveness of -3 (on a log<sub>10</sub> scale), simulation results can be obtained to demonstrate many interesting phenomena. For simplicity in this work, pH effect is ignored and absence of CO<sub>2</sub> are assumed and the effect of H<sub>2</sub>S corrosion is ignored due to low H<sub>2</sub>S concentration. The consumption of sulfate by the bulk biofilm cells is also ignored. The sulfate concentration in the bulk fluid phase is assumed to be constant. Figure 2 shows that mass transfer resistance becomes increasingly important over time. The resistance ratio at time zero is 0.03 (charge transfer control), and at day 365 it becomes 162 (mass transfer control). This fact is manifested in Figure 3 indicating that the corrosion rate decreases quickly initially because the biofilm thickness has increased significantly. The percentage increase of biofilm thickness slows down and thus the further reduction of corrosion rate is decelerated. Figure 3 also shows the pit depth increase over time. The pitting corrosion rate is more severe initially when mass transfer resistance is less important. As a pit grows, the local overall thickness of the SRB biofilm increases. For a deep pit, there is a major mass transfer barrier hampering the sulfate migration from the bulk fluid to the pit bottom. Eventually, the growth of all deep pits will be severely limited by this. It is easy for the model to demonstrate that the growth of all deep pits has mass transfer control because it is difficult for any corrosive

chemical to reach the pit bottom regardless how aggressive a biofilm is able to catalyze surface reactions.

Figure 4 shows that the corrosion potential decreases over time corresponding to a decreasing corrosion rate. As expected, the corrosion potential values are between the anodic and cathodic equilibrium potentials. Sulfate concentration is important in this model for mass transfer controlled cases. Increased sulfate concentration in the bulk-fluid phase will make more sulfate available for cathodic reduction on the iron and biofilm interface leading to more corrosion. Figure 5 demonstrates this by assuming a constant biofilm aggressiveness. It should be noted that in some real world situations, an increased sulfate concentration will lead to more H<sub>2</sub>S generation. This may lead to the formation of protective FeS films that can slow down corrosion<sup>15</sup>. Short-term laboratory SRB experiments are almost always in the charge transfer control region in which sulfate concentration has little effect on MIC pitting if it is not too low as shown in Figure 5.

Figures 6 and 7 show the simulated potentiodynamic sweep profiles. The intersection point of the anodic and cathodic curves yields the corrosion potential and corrosion current density. In Figure 7, the intersection point is clearly in the almost vertical cathodic curve region on the right in which a large change in corrosion potential has little impact on corrosion current density. This is known as concentration polarization or mass transfer control region in electrochemical kinetics. If the sulfate consumption in the bulk SRB biofilm is not ignored, there will be less sulfate reaching the pit bottom surface for its cathodic reduction, thus reducing the corrosion rate, especially in the later period of time that is mass transfer resistance controlled. This behavior is clearly demonstrated in Figure 8. If the SRB biofilm is thick and the pit is deep, the red dashed line for pit depth growth in Figure 8 can actually become flat because all the sulfate will be consumed before reaching the iron surface. This means the pit is dead.

The dual biofilm model can also cope with SRB in a dead leg situation in which there may be a thick stagnant liquid layer with significant diffusion resistance. The resistance can be lumped into the top biofilm resistance, or replacing it if there is no top biofilm. In the latter case, aqueous sulfate diffusivity should be used for the layer.

## **APPLICATIONS AND LIMITATIONS OF THE BCSR MODEL**

The model can be used to predict MIC pitting progression provided that the BCSR theory applies. If the presence of the biofilm is uncertain, the model can still be used to predict the worst-case scenario. As demonstrated above, many effects on MIC can be studied through simulation. The results presented in this work do not include pH in order to concentrate on the effect of cathodic sulfate reduction. If the pH at the pit bottom is quite acidic, pitting will be more severe due to reduction of proton. The model does not consider the deterioration of biofilm aggressiveness due to increased mass transfer limitation of nutrients such as organic carbons as a pit grows. Because sulfate availability at the cathode is much reduced for deep pits, the lowered biofilm aggressiveness will not be problematic unless it is too low. As a pit grows, the headspace of the pit may be filled with sessile SRB cells, corrosion products, or aqueous solution, or a mixture of any of these. Sulfate diffusivity differs in these different media. The simulation results presented in this work are based on the assumption that the SRB biofilm with fixed thickness moves with the pit bottom and the pit headspace is filled with corrosion products and other debris that have similar sulfate diffusivities as the SRB biofilm.

A newer version of the MIC software is currently under development. It considers effects such as temperature, pH, contribution to corrosion from APB, H<sub>2</sub>S, and possible galvanic effect, etc. A 2-D model may also be considered in a later version of the MIC software.

Future MIC prediction will likely be a three-pronged approach. A risk factor model is needed to predict the likelihood of biofilm formation. This will always be a probabilistic model. A mechanistic model such as the one above is then needed to calculate pitting progression assuming that a corrosive biofilm is present. This provides a worst-case scenario. A biofilm field detection method is needed to detect biofilms and possibly to provide quantitative data for calibrating the mechanistic model, if lab tests are not performed. A new biomarker method based on ultra-sensitive EPS (extracellular polymeric substances) fingerprinting has been proposed to address this issue<sup>8</sup>.

## CONCLUSIONS

A mechanistic MIC model has been developed for practical applications. The model considers charge transfer resistance and mass transfer resistance. It can be calibrated with just a single pitting data point (pit depth vs. time) to obtain the aggressiveness of a particular biofilm. This model points to the future directions of MIC research including lab tests and field data collections. The following conclusions have been obtained from model simulations:

- (1) Pitting rate decreases with time due to increased mass transfer resistance over time,
- (2) charge transfer resistance is dominant initially when pit depth is small,
- (3) mass transfer becomes increasingly important when the pit grows deeper, and
- (4) for a deep pit, mass transfer resistance is always a controlling factor.

## REFERENCES

1. H. A. Videla, L. K. Herrera, "Microbiologically influenced corrosion: looking to the future," *International Microbiology*, Vol.8, pp.169-180, 2005.
2. C. A. H. von Wolzogen Kuhr, I. S. vander Vlugt, "Graphication of cast iron as an electrochemical process in anaerobic soils," *Water*, Vol.18, pp.147-165, 1934.
3. D. Thierry, W. Sand, "Microbially influenced corrosion," In: *Corrosion Mechanisms in Theory and Practice*, P. Marcus, J. Oudar (Eds.), Marcel Dekker, New York, pp.457-499, 1995.
4. J. A. Costello, "Cathodic depolarization by sulfate-reducing bacteria," *South African Journal of Science*, Vol.70, pp.202-204, 1974.
5. J. A. Hardy, "Utilisation of cathodic hydrogen by sulphate-reducing bacteria," *British Corrosion Journal*, Vol.18, pp.190-193, 1983.
6. R. Cord-Ruwisch, F. Widdel, "Corroding iron as a hydrogen source for sulphate reduction in growing cultures of sulphate-reducing bacteria," *Applied Microbiology Biotechnology*, Vol.25, pp.169-174, 1986.
7. B. S. Rajagopal, J. LeGall, "Utilization of cathodic hydrogen by hydrogen-oxidizing bacteria," *Applied Microbiology and Biotechnology*, Vol.31, pp.406-412, 1989.

8. K. Zhao, "Investigation of microbiologically influenced corrosion (MIC) and biocide treatment in anaerobic salt water and development of a mechanistic MIC model," PhD dissertation, Ohio University, Athens, OH, Nov., 2008.
9. H-C. Flemming, G. G. Geesey, *Biofouling and Biocorrosion in Industrial Water Systems*, Springer, Berlin, Heidelberg, 1991.
10. A. K. Marcus, C. I. Torres, B. E. Rittmann, "Conduction-based modeling of the biofilm anode of a microbial fuel cell," *Biotechnology and Bioengineering*, Vol.98 (6), pp.1171-1182, 2007.
11. C. P. L. Grady, "Modeling of biological fixed films - a state of the art review," In: *Fixed Film Biological Process for Wastewater Treatment*, Y. C. Wu, E. D. Smith (Eds), Noyes Data Corporation, New Jersey, pp.75-134, 1983.
12. J. E. Bailey, D. F. Ollis, *Biochemical Engineering Fundamentals*, 2<sup>nd</sup> ed., McGraw-Hill, New York, pp.373-453, 1986.
13. L. S. Fan, R. Leyva-Ramos, K. D. Wisecarver, B. J. Zehner, "Diffusion of phenol through a biofilm grown on activated carbon particles in a draft-tube three-phase fluidized-bed bioreactor," *Biotechnology and Bioengineering*, Vol.35, pp.279-286, 1990.
14. W. Sun, "Kinetics of iron carbonate and iron sulfide scale formation in CO<sub>2</sub>/H<sub>2</sub>S corrosion," PhD dissertation, Ohio University, Athens, OH, Nov., 2006.
15. W. Sun, S. Nescic, "Kinetics of iron sulfide and mixed iron sulfide/carbonate scale precipitation in CO<sub>2</sub>/H<sub>2</sub>S corrosion," Corrosion/06, Paper no.06644, NACE International, Houston, Texas, 2006.



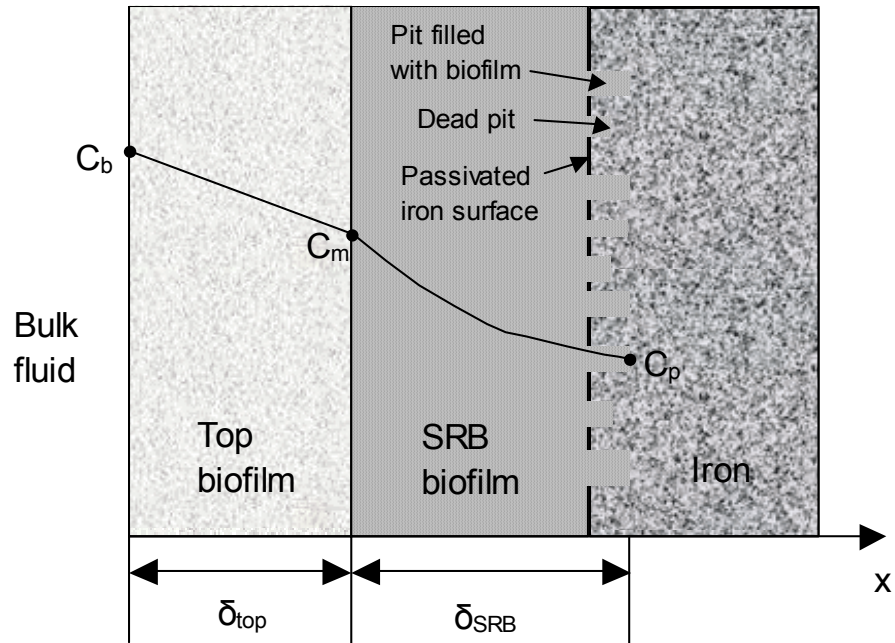


**FIGURE 1– Illustration of mass transfer of sulfate from bulk-fluid phase to pit bottom.**

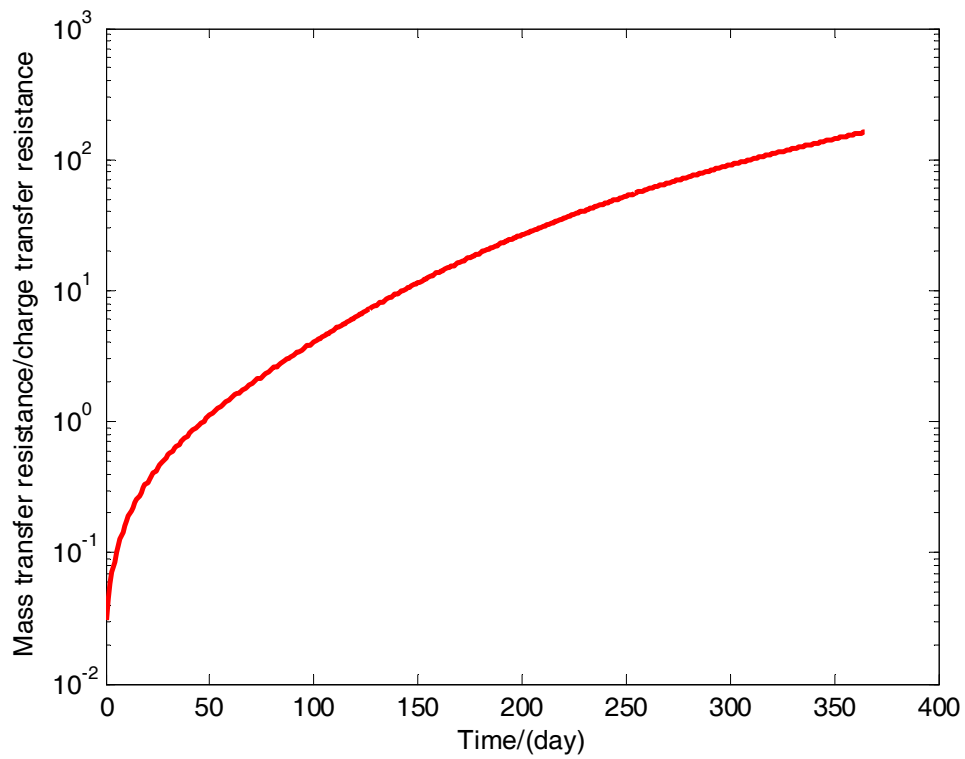


**FIGURE 2 – Simulated corrosion resistance ratio.**

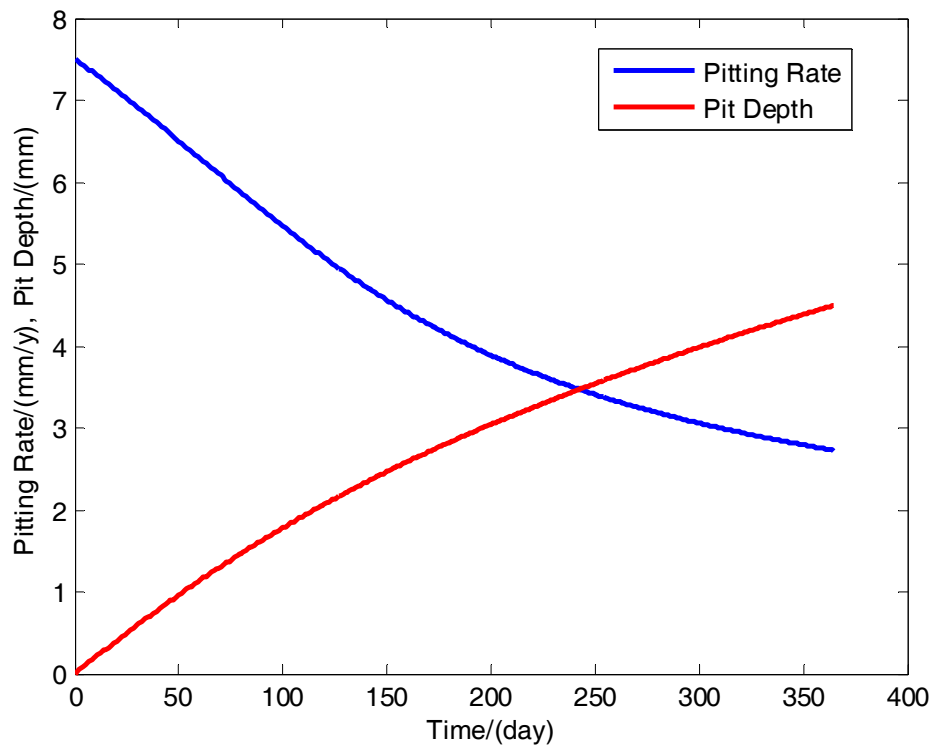


**FIGURE 3 – Simulated corrosion rate and pit depth profiles.**

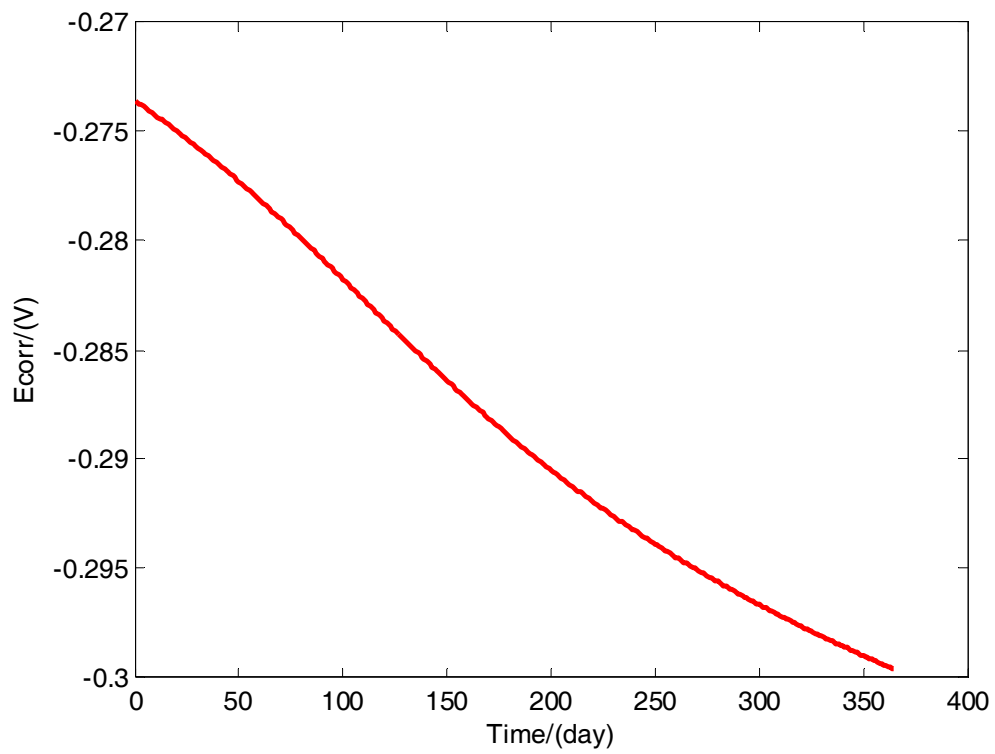


**FIGURE 4 – Simulated corrosion potential profile.**

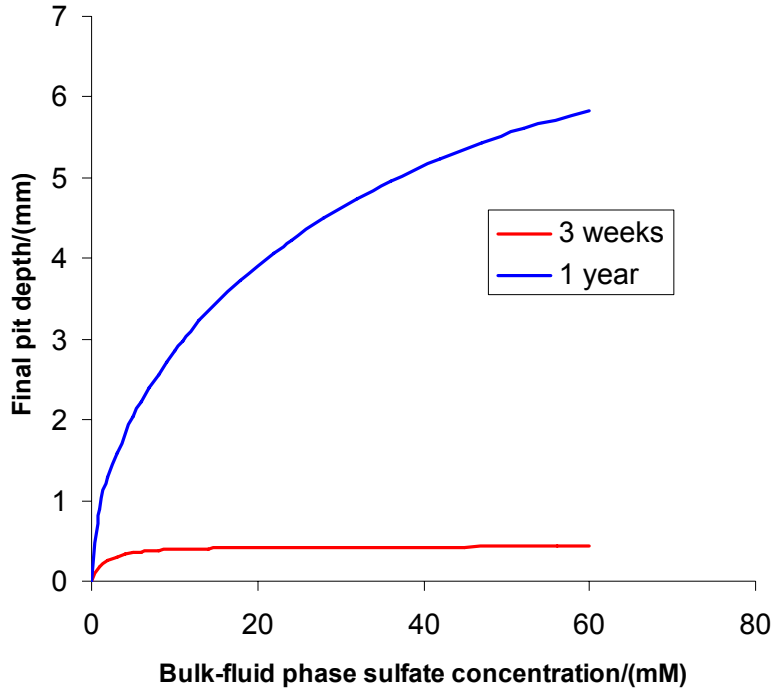


**FIGURE 5 – Simulated effect of sulfate concentration**

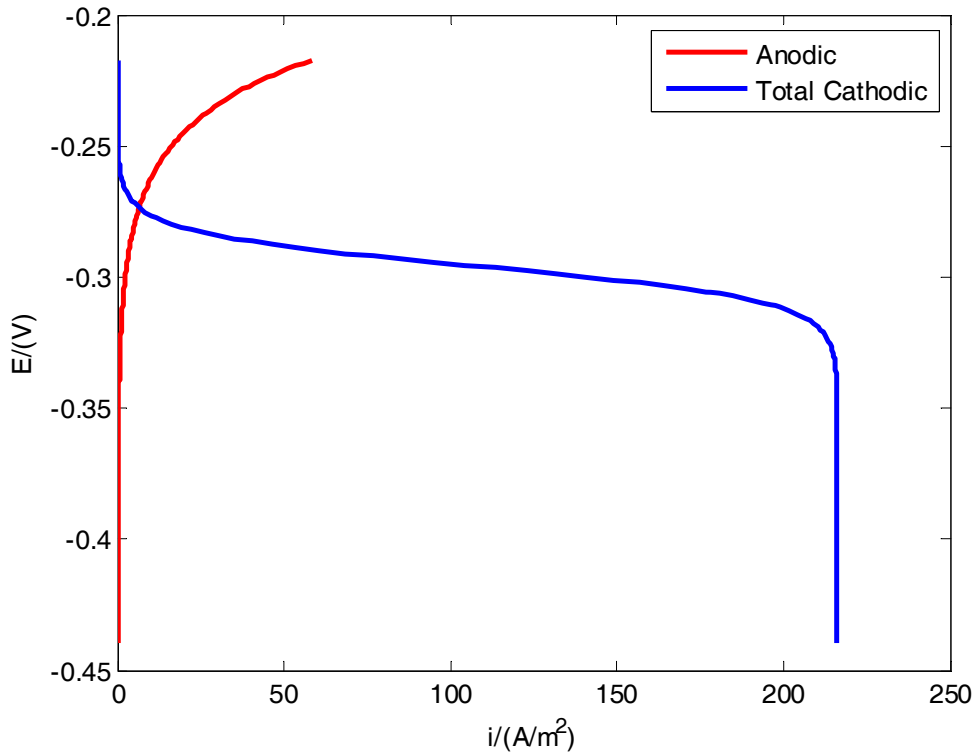


**FIGURE 6 – Simulated potentiodynamic sweep profiles at time zero**

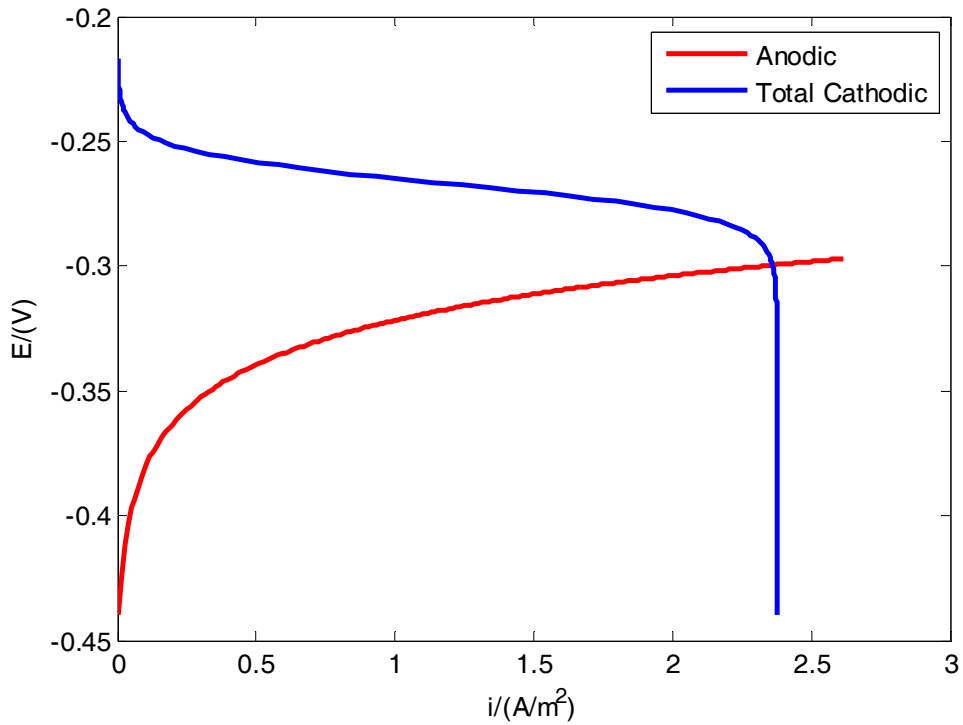


**FIGURE 7 – Simulated potentiodynamic sweep profiles at day 365.**

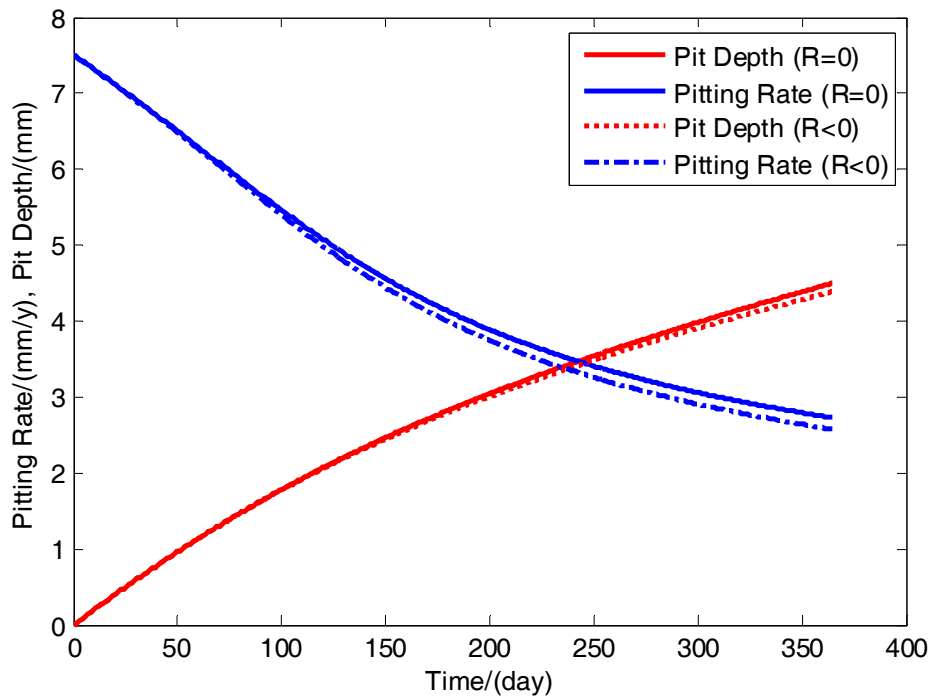


**FIGURE 8 – Effect of sulfate consumption by the bulk SRB biofilm. (Solid lines are the same as in Figure 3. Dashed lines are from simulation using the same data as in Figure 3 except  $R = -5 \times 10^{-3} \text{ mol}/(\text{m}^3\text{s})$ .)**